

## Toward Remote Physical-Model-Based Fault Localization in Transmission-Line Networks

P. DEL HOUGNE\*

*Univ. Rennes, CNRS, IETR-UMR 6164, F-35000 Rennes, France*

Doi: [10.12693/APhysPolA.144.441](https://doi.org/10.12693/APhysPolA.144.441)

\*e-mail: [philipp.del-hougne@univ-rennes1.fr](mailto:philipp.del-hougne@univ-rennes1.fr)

We analytically derive the updates of a transmission-line network's interaction matrix and scattering matrix as a consequence of a fault (an interrupted transmission line). We find that the fault alters not only the direct coupling between the two nodes that were previously connected by the faulty cable, but that the fault also alters these nodes' self-interactions in a non-trivial manner. Given the network's topology, it is then possible to *remotely* localize the fault on the faulty cable based on measurements of the faulty network's scattering coefficient(s). Our analytical expressions make it possible to efficiently calculate the expected scattering matrix for different fault locations (orders of magnitude faster than a brute-force evaluation). We report a simple demonstration for which we assume to know the network's topology as well as which cable is faulty; we identify the location of the fault on the faulty cable by comparing the broadband scattering coefficient(s) swept across candidate fault locations to the one(s) measured on the faulty network.

topics: transmission-line network, fault localization, physical-model-based remote sensing, isospectral reduction

### 1. Introduction

In a simple cable, a fault is easily localized via time-domain analysis of the cable's reflection or transmission coefficient. In this paper, we are interested in the more challenging problem of localizing a fault in a cable that is part of a complex transmission-line network. Thus, we cannot probe the cable in isolation nor directly. We can only probe the cable remotely via asymptotic scattering channels connecting the network to the outside world. In general, asymptotic scattering channels are not directly connected to the faulty cable of interest.

Fault localization in a complex transmission-line network can be understood as a sensing problem inside a complex scattering medium. On the one hand, reverberation in such a complex system can drastically enhance the achievable resolution because it boosts the wave's sensitivity to the perturbation of interest. Indeed, we recently demonstrated a direct link between the resolution with which an object can be localized inside a chaotic cavity and the dwell time of the wave inside the cavity [1]. The chaotic cavity acts essentially like a generalized interferometer, and the resulting interferometric sensitivity can yield orders of magnitude finer resolution than in free space. Deeply sub-wavelength resolution without capturing evanescent waves is thereby feasible [1]. On the other hand, data analysis inevitably must take into account the complexity of the specific system. In [1], the exact

geometry and material composition of the chaotic cavity were unknown such that a calibration dataset had to be measured to characterize the specific system's complexity. In contrast, in the present case of a transmission-line network, the topology is usually known, so that its complexity can be taken into account without the need for calibration measurements.

The considered problem of remotely localizing a network fault is of practical importance, for instance, to diagnose line outages in large networks. Currently, such problems are often studied under simplifying assumptions (e.g., using DC approximation of AC power flow models) and assuming that a line outage simply removes the line from the network topology [2]. Our analytical calculations in the present paper based on a physical model suggest that a fault additionally impacts (in a significant and non-trivial manner) the self-interactions of the nodes that were connected by the faulty line.

Meanwhile, we note that other physics-based remote-sensing approaches for transmission-line networks are currently being explored in the literature. For example, [3] considers the case of an initial network being split at various edges and nodes into two networks; it is shown in [3] that by determining the networks' Euler characteristic from scattering measurements [4], one can determine at how many edges and nodes the initial network was split — even without knowing its topology.

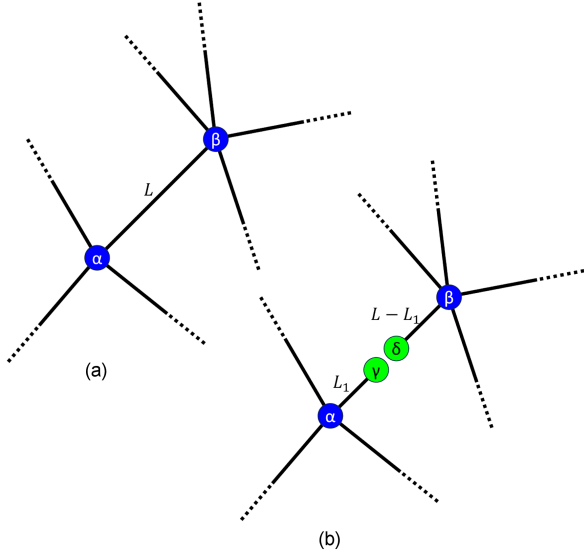


Fig. 1. Considered fault: the cable linking nodes  $\alpha$  and  $\beta$  is interrupted (cut) at a distance  $L_1$  from  $\alpha$ , creating two new nodes  $\gamma$  and  $\delta$ . The sketches show (a) an intact cable and (b) a faulty cable of interest within a larger transmission-line network.

Related to the present paper is also a “differential DORT” technique<sup>†</sup> for the detection of *soft* faults in complex wire networks that is similarly based on measuring the scattering matrix of the intact and faulty network, as well as knowledge of the network topology [5]. The signal processing in this “differential DORT” technique consists in identifying the wavefront that focuses on the fault (hence the term “DORT” in the technique’s name), computing the field distribution within the network, and comparing it to the baseline field distribution (hence the term “differential” in the technique’s name). However, as pointed out in [5], this differential approach relies on the Born approximation (i.e., the amount of power scattered by the fault is small, so there is no significant portion of the wave energy that interacts with the fault more than once). Therefore, the technique is limited to *soft* faults, which only weakly perturb the network. In contrast, the present paper considers *hard* faults, which are open circuits. Hence, many interactions with the fault occur, and, in fact, the resolution improves with the number of interactions [1].

In the present paper, we derive an analytical expression for how a fault alters the interaction matrix of a given network and thereby the observable scattering coefficient(s). We numerically validate the derived expressions and demonstrate their application to remote physical-model-based fault localization.

<sup>†</sup>DORT — decomposition of the time reversal operator

## 2. Background

In this section, we recall the well-established background on wave scattering in a transmission-line network on which our subsequent analysis builds.

A transmission-line network, also known as a “quantum graph” [6–8], can be understood as composed of non-resonant scattering entities (its nodes, i.e., junctions) that have certain couplings between each other (its bonds, i.e., cables) and with the outside world (asymptotic scattering channels). Let us consider a system composed of  $n$  nodes of which  $m \leq n$  are directly connected to the asymptotic scattering channel; we assume that each asymptotic scattering channel is non-dispersively coupled to exactly one node.

The considered transmission-line networks are also known as Neumann quantum graphs, and [7, 9, 10] derived an exact expression relating the system’s scattering matrix  $S \in \mathbb{C}^{m \times m}$  to the network topology

$$S = I_m - 2i W^\dagger \frac{1}{H + iWW^\dagger} W. \quad (1)$$

The matrices involved in (1) are defined as follows:

1.  $I_m \in \mathbb{B}^{m \times m}$  is the  $m \times m$  identity matrix.
2.  $W \in \mathbb{B}^{n \times m}$  is the coupling matrix describing the coupling between each node and each asymptotic scattering channel. If the  $i$ -th meta-atom is connected to the  $j$ -th asymptotic scattering channel, the  $(i, j)$ -th entry of  $W$  is unity; otherwise, it is zero.
3.  $H \in \mathbb{R}^{n \times n}$  is the interaction matrix of the transmission-line network. Its  $(i, j)$ -th entry is defined as follows

$$H_{i,j} = \begin{cases} -\sum_{l \neq i} C_{i,l} \cot(kL_{i,l}), & \text{if } i = j, \\ C_{i,j} \csc(kL_{i,j}), & \text{otherwise.} \end{cases} \quad (2)$$

Here,  $C_{i,j}$  is unity if the nodes indexed  $i$  and  $j$  are directly connected, and zero otherwise;  $L_{i,j}$  is the length of the cable connecting the nodes indexed  $i$  and  $j$ ;  $k$  is the wavenumber. In the present paper, we limit ourselves to reciprocal bonds, so  $H$  is a symmetric matrix. Moreover, its dependence on the wavenumber implies that  $H$ , and therefore also  $S$ , are frequency dependent.

## 3. Physics-compliant fault model

The fault considered in this paper is illustrated in Fig. 1, where the cable of length  $L$  linking nodes  $\alpha$  and  $\beta$  is cut at a distance  $L_1$  from  $\alpha$ . This fault implies that the direct link between nodes  $\alpha$  and  $\beta$  is interrupted, but this fault is *not* equivalent to just removing the cable between  $\alpha$  and  $\beta$ . The waves will still travel along the faulty cable and will be

$$\mathbf{H}_1^{\text{red}} = \mathbf{H}_0 + \underbrace{\Delta}_{\begin{array}{c} \dots \\ \alpha \ \beta \\ \vdots \\ \alpha \ \beta \end{array}} - \underbrace{\mathbf{X}}_{\begin{array}{c} \gamma \ \delta \\ \alpha \ \beta \end{array}} \underbrace{\mathbf{Z}^{-1}}_{\begin{pmatrix} \gamma & \delta \\ \alpha & f \\ \beta & g \end{pmatrix}^{-1}} \underbrace{\mathbf{Y}}_{\begin{array}{c} \gamma \ \delta \\ \alpha \ \beta \end{array}} = \mathbf{H}_0 + \underbrace{\Gamma}_{\begin{array}{c} \dots \\ \alpha \ \beta \\ \vdots \\ \alpha \ \beta \end{array}}$$

$a = \cot(kL) - \cot(kL_1)$
$b = -\csc(kL)$
$c = \cot(kL) - \cot(k(L - L_1))$
$d = \csc(kL_1)$
$e = \csc(k(L - L_1))$
$f = -\cot(kL_1)$
$g = -\cot(k(L - L_1))$
$p = a - d^2/f$
$q = c - e^2/g$

Fig. 2. Fault-induced update of the interaction matrix in the reduced  $n \times n$  basis. The update concerns  $2 \times 2$  block of the interaction matrix involving nodes  $\alpha$  and  $\beta$ .

reflected by the fault, which we assume to be an open-circuit end. Therefore, the physics-compliant fault model consists of two modifications of the original network topology:

1. Removal of the cable linking nodes  $\alpha$  and  $\beta$ .
2. Creation of two new nodes,  $\gamma$  and  $\delta$ , which are directly connected to  $\alpha$  and  $\beta$  via cables of length  $L_1$  and  $L - L_1$ , respectively.

Let us denote by  $H_0$  and  $S_0$  the interaction matrix and scattering matrix of the intact transmission-line network of interest, respectively. Assuming the network topology is known,  $H_0$  and  $S_0$  are also known analytically. When a fault appears, the faulty network is described by  $H_1$  and  $S_1$ . Note that the dimensions of  $H_1$  are  $(n+2) \times (n+2)$  because of the two new nodes  $\gamma$  and  $\delta$ . (Of course, the dimensions of both  $S_1$  and  $S_0$  are  $n \times n$ .)

We assume that we know (i) the network topology and (ii) which cable is faulty, and we seek to localize the fault on the faulty cable by estimating  $L_1$ . Our next goal is hence to find an analytical expression for  $\Delta S = S_1 - S_0$  as a function of the sought-after parameter  $L_1$ .

#### 4. Interaction matrix update due to fault

As a first step, we seek to identify in this section how the interaction matrix of our network must be updated to account for the fault. Without loss of generality, we index the nodes of the intact network such that  $\alpha$  and  $\beta$  have indices  $(n-1)$  and  $n$ , respectively.

So far, we have considered the interaction matrix always in the canonical basis, where its dimensions directly correspond to the number of nodes. However, there are equivalent representations reduced to a subset of nodes. Indeed, nodes that are not directly connected to asymptotic scattering channels can equivalently be understood as merely being a non-local coupling mechanism between the remaining nodes. Mathematically, such a reduced-basis representation is based on the block matrix inversion lemma. Calculations of reduced-basis interaction matrices were presented in contexts ranging from tight-binding network engineering [11]

to isospectral graph reduction [12]. In particular, we have recently used them to achieve covert symmetry-based wave scattering control by encoding the symmetry in the non-local interactions between ‘‘primary’’ meta-atoms such that the symmetry is ‘‘hidden’’, i.e., the symmetry is only apparent in a reduced basis but not in the canonical basis [13]; very recently, we also used a reduced-basis representation to formulate and calibrate compact physics-compliant models of massively parametrized complex media such as ‘‘smart’’ radio environments [14, 15].

In the present context, the two fault-induced new nodes,  $\gamma$  and  $\delta$ , are certainly not directly connected to any asymptotic scattering channel (they have only one connection to  $\alpha$  or  $\beta$ , respectively). Therefore, we can find an equivalent representation of  $H_1$  in the basis reduced to the  $n$  initial nodes. We begin by writing  $H_1$  in block form

$$\mathbf{H}_1 = \begin{bmatrix} \mathbf{H}_{1,n} & \mathbf{X} \\ \mathbf{Y} & \mathbf{Z} \end{bmatrix}, \quad (3)$$

where  $\mathbf{H}_{1,n} \in \mathbb{R}^{n \times n}$ ,  $\mathbf{X} \in \mathbb{R}^{n \times 2}$ ,  $\mathbf{Y} \in \mathbb{R}^{2 \times n}$ , and  $\mathbf{Z} \in \mathbb{C}^{2 \times 2}$ . Then, the reduced-basis representation of  $H_1$  is

$$\mathbf{H}_1^{\text{red}} = \mathbf{H}_{1,n} - \mathbf{X}\mathbf{Z}^{-1}\mathbf{Y}. \quad (4)$$

Since our goal is to express  $\mathbf{H}_1^{\text{red}}$  as an update of  $\mathbf{H}_0$ , we introduce  $\Delta = \mathbf{H}_{1,n} - \mathbf{H}_0$ . Now, we can formulate the impact of the fault as an update of the original interaction matrix

$$\mathbf{H}_1^{\text{red}} = \mathbf{H}_0 + \Delta - \mathbf{X}\mathbf{Z}^{-1}\mathbf{Y} = \mathbf{H}_0 + \Gamma. \quad (5)$$

Next, we seek to define the entries of  $\Gamma = \Delta - \mathbf{X}\mathbf{Z}^{-1}\mathbf{Y}$  in terms of  $L_1$ . This procedure is illustrated in Fig. 2. The only non-zero entries of  $\Delta$  are the ones in its bottom right  $2 \times 2$  block

$$\begin{aligned}
 \Delta_{n-1,n-1} &= a = \cot(kL) - \cot(kL_1), \\
 \Delta_{n-1,n} &= \Delta_{n,n-1} = b = -\csc(kL), \\
 \Delta_{n,n} &= c = \cot(kL) - \cot(k(L - L_1)).
 \end{aligned} \quad (6)$$

The only non-zero entries of  $\mathbf{X} = \mathbf{Y}^T$  are the following two

$$\begin{aligned}
 X_{n-1,1} &= Y_{1,n-1} = d = \csc(kL_1), \\
 X_{n,2} &= Y_{2,n} = e = \csc(k(L - L_1)).
 \end{aligned} \quad (7)$$

The entries of  $Z$  are as follows

$$\begin{aligned} Z_{1,1} &= f = -\cot(kL_1), \\ Z_{1,2} &= Z_{2,1} = 0, \\ Z_{2,2} &= g = -\cot(k(L - L_1)). \end{aligned} \quad (8)$$

Ultimately, we find that only the bottom right  $2 \times 2$  block of  $\Gamma$  is non-zero, i.e.,

$$\begin{aligned} \Gamma_{n-1,n-1} &= p = a - \frac{d^2}{f} = \cot(kL) - \cot(kL_1) \\ &\quad + \frac{(\csc(kL_1))^2}{\cot(kL_1)}, \\ \Gamma_{n-1,n} &= \Gamma_{n,n-1} = b = -\csc(kL), \\ \Gamma_{n,n} &= q = c - \frac{e^2}{g} = \cot(kL) - \cot(k(L - L_1)) \\ &\quad + \frac{(\csc(k(L - L_1)))^2}{\cot(k(L - L_1))}. \end{aligned} \quad (9)$$

Therefore, the fault has not only removed the direct coupling between  $\alpha$  and  $\beta$ , but it has also changed the self-interactions of  $\alpha$  and  $\beta$  in a non-trivial way. One possible interpretation is that in the reduced basis,  $\alpha$  and  $\beta$  are now resonant because they have a cable of length  $L_1$  or  $L - L_1$ , respectively, with open-circuit termination attached to them.

## 5. Scattering matrix update due to fault

In the previous section, we expressed the impact of the fault as an update (parametrized by  $L_1$ ) of the interaction matrix. In this section, we now evaluate how the scattering matrix of the network is updated due to the fault. As seen in (1), to go from the interaction matrix  $H$  to the scattering matrix  $S$ , the matrix  $G = H + iWW^\dagger$  must be inverted. We define

$$\begin{aligned} G_1 &= H_1^{\text{red}} + iWW^\dagger = H_0 + \Gamma + iWW^\dagger = \\ &G_0 + \Gamma = G_0 + UDV, \end{aligned} \quad (10)$$

where

$$U = \begin{bmatrix} 0_{n-2,2} \\ Q \end{bmatrix} \quad \text{and} \quad V = \begin{bmatrix} 0_{n-2,2}^T & Q^{-1} \end{bmatrix}, \quad (11)$$

and where  $QDQ^{-1}$  is the eigendecomposition of the bottom right  $2 \times 2$  block of  $\Gamma$ , and  $0_{n-2,2}$  is a  $(n-2) \times 2$  matrix of zeros.

Based on the Woodbury matrix identity, we obtain

$$G_1^{-1} = G_0^{-1} - G_0^{-1}U(D^{-1} + VG_0^{-1}U)^{-1}VG_0^{-1} \quad (12)$$

and hence

$$\begin{aligned} S_1 &= I - 2iW^\dagger G_1^{-1}W = \\ &S_0 + 2iW^\dagger \left[ G_0^{-1}U(D^{-1} + VG_0^{-1}U)^{-1}VG_0^{-1} \right] W. \end{aligned} \quad (13)$$

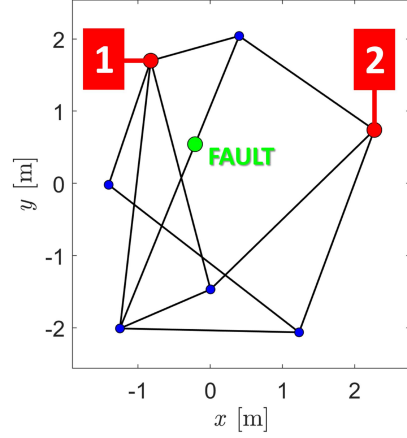


Fig. 3. Considered random transmission-line network. Each of the two red nodes is directly connected to one asymptotic scattering channel. The location of the fault, at which the faulty cable is interrupted, is highlighted in green.

Next, we seek to express  $Q$  and  $D$  in terms of  $L_1$  so that we can analytically relate the change of the observable scattering coefficient(s) to  $L_1$ . The analytical eigendecomposition of the bottom right  $2 \times 2$  block of  $\Gamma$  yields

$$\begin{aligned} Q &= \begin{bmatrix} \frac{-(q-p+z)}{2b} & \frac{p-q+z}{2b} \\ 1 & 1 \end{bmatrix}, \\ D &= \text{diag} \left( \left[ \frac{p+q-z}{2} \quad \frac{p+q+z}{2} \right] \right), \end{aligned} \quad (14)$$

where  $z = \sqrt{p^2 - 2pq + q^2 + 4b^2}$ , and the  $\text{diag}(\cdot)$  operator constructs a diagonal matrix from a vector.

Equations (13) and (14) are the key result of the present paper, analytically relating the update of  $S$  due to the fault to  $L_1$ .

## 6. Application to an example network

In this section, we consider a specific example network (i) to validate the key result of our analytical calculations (i.e., (13)) and (ii) to demonstrate its use for fault localization.

### 6.1. Numerical validation of (13)

We consider the example random transmission-line network shown in Fig. 3. Two asymptotic scattering channels are connected to the network, and one of the network's inner cables is interrupted by a fault. We assume the wave speed to be 70 % of the speed of light in free space.

In Fig. 4 we plot the frequency-dependent scattering coefficients of the intact (blue) and faulty (red) networks. The fault altered the network's scattering matrix very significantly. The blue and red

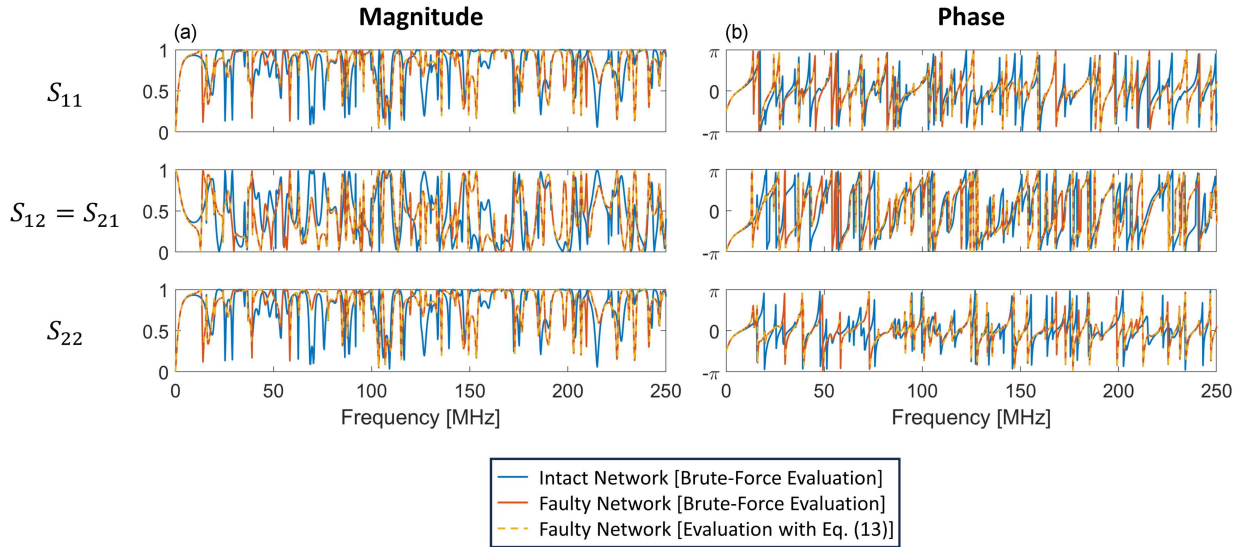


Fig. 4. Comparison of the frequency-dependent scattering coefficients in terms of magnitude (a) and phase (b) for the intact network (blue), the faulty network (red), and the faulty network evaluated with (13) (yellow).

curves are evaluated with the brute-force approach from (2). However, in the case of the faulty network, the scattering coefficients can be more efficiently evaluated as updates of the intact network’s scattering coefficients using (13), yielding the yellow lines in Fig. 4. The agreement between red and yellow lines validates the analytical expression from (13).

### 6.2. Remote model-based fault localization

The faulty network’s transmission coefficient  $S_{21}(f)$  is a wave fingerprint of the fault’s location [1, 16, 17]. Given (13), we can now analytically calculate the expected transmission spectra for different candidate fault locations  $L_1$ , in order to identify the one that best explains the measured  $S_{21}(f)$  of the faulty network.

For the sake of simplicity, we assume negligible measurement noise. For our analysis, we restrict ourselves to a rather small (arbitrarily chosen) frequency interval,  $37.3 < f < 49.8$  MHz, with 50 linearly spaced frequency points. We consider 1000 linearly spaced candidate values of  $L_1$  between zero and the length of the cable connecting  $\alpha$  and  $\beta$  in the intact network. For each candidate value of  $L_1$ , we compute the correlation coefficient of the transmission spectrum with that measured on the faulty network. Our estimate of  $L_1$  is then simply the candidate value with the highest correlation coefficient. Our results displayed in Fig. 5 provide an accurate estimate of  $L_1$ , orders of magnitude better than the smallest measured wavelength (4.2 m for 49.8 MHz).

Of course, the data analysis method can be refined to endow it with robustness against measurement noise [1] and/or environmental perturbations [17], for example by training an artificial neural network for the wave fingerprint identification,

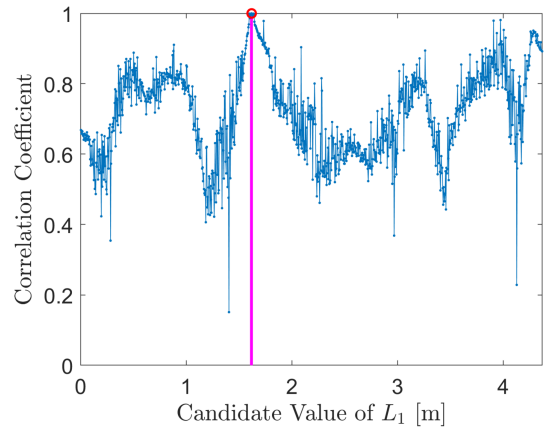


Fig. 5. Demonstration of remote model-based fault localization for the faulty network from Fig. 3. The vertical magenta-colored line indicates the ground-truth value of  $L_1$ .

as reported in [1, 17] for localization in a chaotic cavity. The application of these techniques to the localization of faults in transmission-line networks is left for future work. The main purpose of the present work is to demonstrate that in the case of a transmission-line network, wave-fingerprint-based localization techniques can be applied using an efficient physics-compliant model, instead of having to collect experimental calibration data.

## 7. Conclusions

To summarize, we have derived an analytical expression for the update of a transmission-line network’s scattering matrix due to a fault. We found that besides removing the direct connection

between two nodes, a fault also significantly alters the self-interactions of these two nodes in a rather complicated manner. Using the derived physics-compliant model, we *remotely* localized the fault in an example random network with high accuracy based on the faulty network's transmission spectrum. Looking forward, the signal-processing aspects of the methodology can be refined to remove the need for knowing which cable is the faulty one, and to be resilient against noise and environmental perturbations. Naturally, experimental validations at various scales are also envisioned.

### References

- [1] M. del Hougne, S. Gigan, P. del Hougne, *Phys. Rev. Lett.* **127**, 043903 (2021).
- [2] Y. Zhao, J. Chen, H.V. Poor, *IEEE Trans. Smart Grid.* **11**, 555 (2019).
- [3] O. Farooq, A. Akhshani, M. Bialous, S. Bauch, M. Lawniczak, L. Sirko, *Phys. Scr.* **98**, 024005 (2023).
- [4] M. Lawniczak, P. Kurasov, S. Bauch, M. Bialous, V. Yunko, L. Sirko, *Phys. Rev. E* **101**, 052320 (2020).
- [5] L. Abboud, A. Cozza, L. Pichon, *IEEE Trans. Veh. Technol.* **62**, 1010 (2013).
- [6] T. Kottos, U. Smilansky, *Phys. Rev. Lett.* **79**, 4794 (1997).
- [7] T. Kottos, U. Smilansky, *J. Phys. A* **36**, 3501 (2003).
- [8] O. Hul, S. Bauch, P. Pakoński, N. Savyt-skyy, K. Zyczkowski, L. Sirko, *Phys. Rev. E* **69**, 056205 (2004).
- [9] C. Texier, G. Montambaux, *J. Phys. A* **34**, 10307 (2001).
- [10] P. Kuchment, *Waves Random Media* **14**, S107 (2003).
- [11] S. Longhi, *Phys. Rev. A* **93**, 022102 (2016).
- [12] L. Bunimovich, B. Webb, *Isospectral Transformations*, Springer Monogr. Math., 2014.
- [13] J. Sol, M. Röntgen, P. del Hougne, *Adv. Mater.* **2023**, 2303891 (2023).
- [14] H. Prod'homme, P. del Hougne, [arXiv:2306.00244](https://arxiv.org/abs/2306.00244), 2023, in press at *IEEE Commun. Lett.*
- [15] J. Sol, H. Prod'homme, L. Le Magoarou, P. del Hougne, [arXiv:2308.02349](https://arxiv.org/abs/2308.02349), 2023.
- [16] P. del Hougne, M.F. Imani, M. Fink, D.R. Smith, G. Lerosey, *Phys. Rev. Lett.* **121**, 063901 (2018).
- [17] P. del Hougne, *Phys. Rev. Research* **2**, 043224 (2020).